

The role of the radiative corrections in ν interactions

Francesca Dordei, INFN Cagliari
 francesca.dordei@cern.ch



NOW 2024, 7th September 2024, Otranto

Momentum dependent flavor radiative corrections to the coherent elastic neutrino-nucleus scattering for the neutrino charge-radius determination

M. Atzori Corona^{a,b}, M. Cadeddu^b, N. Cargioli^{a,b}, F. Dordei^b and C. Giunti^{b,c}

^a*Dipartimento di Fisica, Università degli Studi di Cagliari, Complesso Universitario di Monserrato - S.P. per Sestu Km 0.700, 09042 Monserrato (Cagliari), Italy*

^b*Istituto Nazionale di Fisica Nucleare (INFN), Sezione di Cagliari, Complesso Universitario di Monserrato - S.P. per Sestu Km 0.700, 09042 Monserrato (Cagliari), Italy*

^c*Istituto Nazionale di Fisica Nucleare (INFN), Sezione di Torino, Via P. Giuria 1, I-10125 Torino, Italy*

E-mail: mattia.atzori@ca.infn.it, matteo.cadeddu@ca.infn.it, nicola.cargioli@ca.infn.it, francesca.dordei@cern.ch, carlo.giunti@to.infn.it

ABSTRACT: Despite being neutral particles, neutrinos can have a non-zero charge radius, which represents the only non-null neutrino electromagnetic property in the standard model theory. Its value can be predicted with high accuracy and its effect is usually accounted for through the definition of a radiative correction affecting the neutrino couplings to electrons and nucleons at low energy, which results effectively in a shift of the weak mixing angle. Interestingly, it introduces a flavour-dependence in the cross-section. Exploiting available neutrino-electron and coherent elastic neutrino-nucleus scattering (CE ν NS) data, there have been many attempts to measure experimentally the neutrino charge radius. Unfortunately, the current precision allows one to only determine constraints on its value. In this work, we discuss how to properly account for the neutrino charge radius in the CE ν NS cross-section including the effects of the non-null momentum-transfer in the neutrino electromagnetic form factor, which have been usually neglected when deriving the aforementioned limits. We apply the formalism discussed to a re-analysis of the COHERENT cesium iodide and argon samples and the NCC-1701 germanium data from the Dresden-II nuclear power plant. We quantify the impact of this correction on the CE ν NS cross-section and we show that, despite being small, it can not be neglected in the analysis of data from future high-precision experiments. Furthermore, this momentum dependence can be exploited to significantly reduce the allowed values for the neutrino charge radius determination.

KEYWORDS: Non-Standard Neutrino Properties, Neutrino Interactions

ARXIV EPRINT: [2402.16709](https://arxiv.org/abs/2402.16709)

BASED ON
JHEP05(2024)271 [ARXIV:2402.16709]

[https://link.springer.com/article/10.1007/JHEP05\(2024\)271](https://link.springer.com/article/10.1007/JHEP05(2024)271)



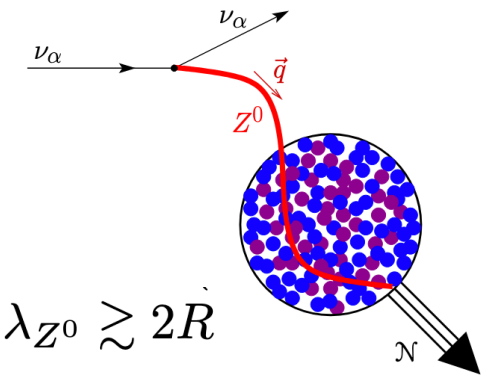
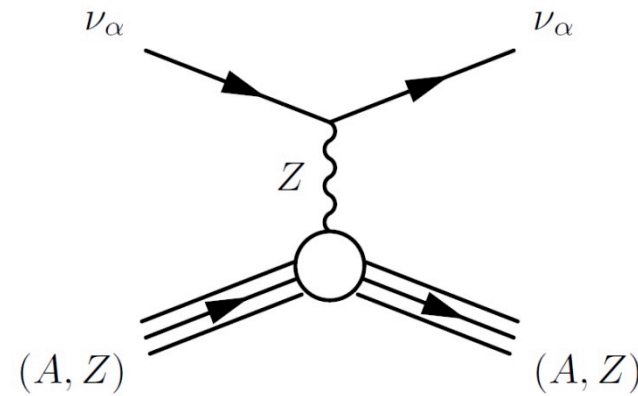
Done in collaboration with: **M. Atzori Corona, M. Cadeddu, N. Cargioli, C. Giunti**

CE ν NS

- **Coherent Elastic Neutrino-Nucleus Scattering (CE ν NS):** A neutrino scatters off a nucleus via exchange of a Z boson, and the nucleus recoils as a whole

$$\nu_\alpha + (A, Z) \rightarrow \nu_\alpha + (A, Z)$$

- Predicted in 1974 by Freedman
- Low momentum transfer (MeV scale) needed \rightarrow MeV scale neutrinos required! It **took more than 40 years to finally measure** nuclear recoils originating from this neutrino interaction!



$$\lambda_{Z^0} \gtrsim 2R$$

For a recent review see
EPL 143 (2023) 3, 34001

PHYSICAL REVIEW D

VOLUME 9, NUMBER 5

1 MARCH 1974

Coherent effects of a weak neutral current

Daniel Z. Freedman[†]

National Accelerator Laboratory, Batavia, Illinois 60510

and Institute for Theoretical Physics, State University of New York, Stony Brook, New York 11790

(Received 15 October 1973; revised manuscript received 19 November 1973)

If there is a weak neutral current, then the elastic scattering process $\nu + A \rightarrow \nu + A$ should have a sharp coherent forward peak just as $e + A \rightarrow e + A$ does. Experiments to observe this peak can give important information on the isospin structure of the neutral current. The experiments are very difficult, although the estimated cross sections (about 10^{-38} cm² on carbon) are favorable. The coherent cross sections (in contrast to incoherent) are almost energy-independent. Therefore, energies as low as 100 MeV may be suitable. Quasi-coherent nuclear excitation processes $\nu + A \rightarrow \nu + A^*$ provide possible tests of the conservation of the weak neutral current. Because of strong coherent effects at very low energies, the nuclear elastic scattering process may be important in inhibiting cooling by neutrino emission in stellar collapse and neutron stars.

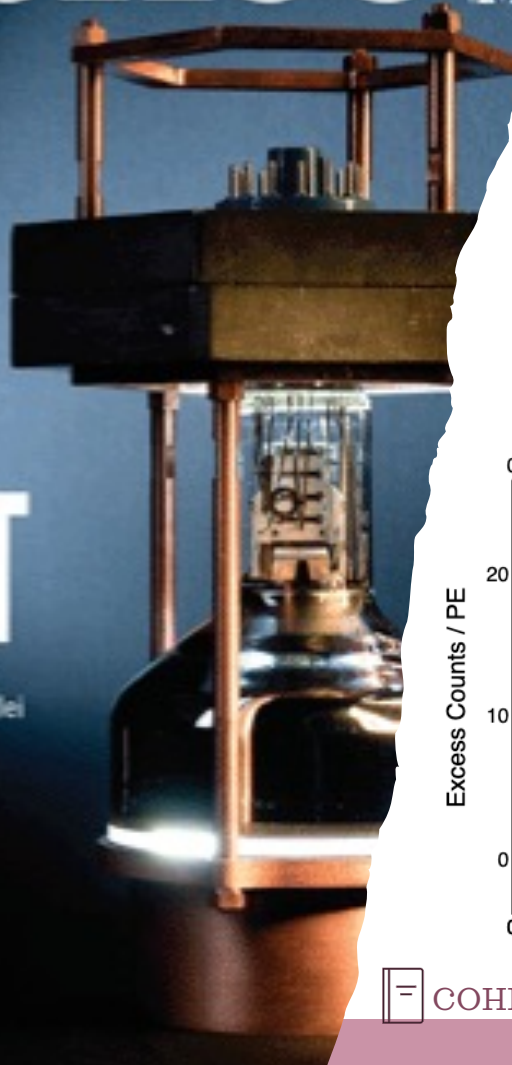
Our suggestion may be **an act of hubris**, because **the inevitable constraints of interaction rate, resolution, and background pose grave experimental difficulties for elastic neutrino-nucleus scattering.**

We will discuss these problems at the end of this note, but first we wish to present the theoretical ideas relevant to the experiments.

Science

SPOTTING A GHOST

A compact detector spies neutrinos scattering from nuclei
pp. 1098 & 1123

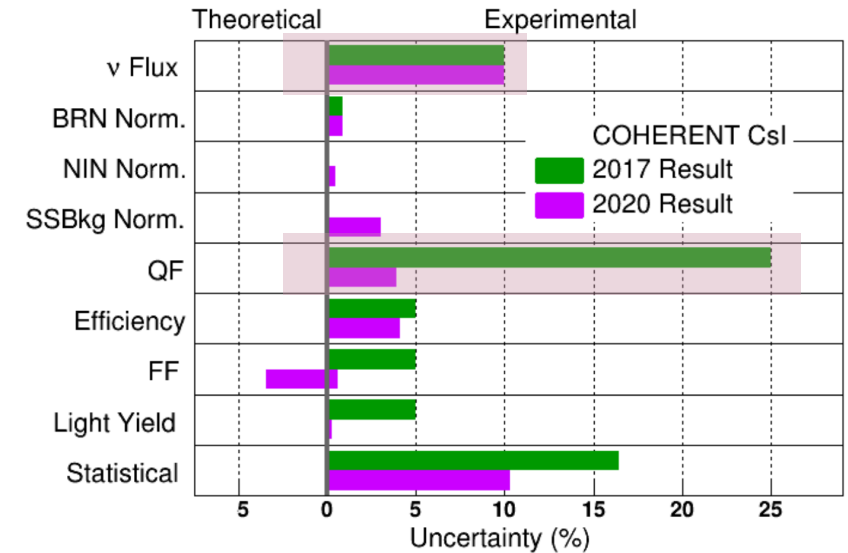
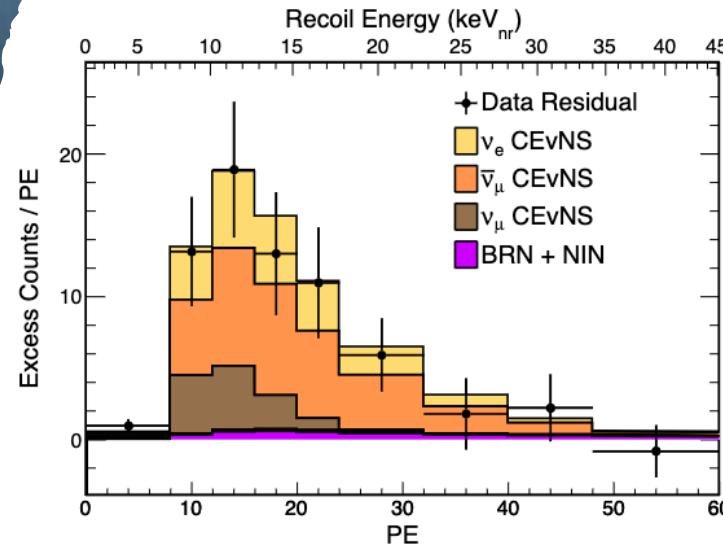


Leading actor I



See D. Pershey talk

- Full CEνNS dataset with 14.6 kg CsI scintillating crystal and neutrinos from πDAR
- **306 ± 20 CEνNS** events: 11.6σ significance
- To be compared with prediction: **333±11(th)+42(ex)** events
- ✓ Result is consistent with SM prediction at 1σ
- ✓ Double exposure wrt 2017 and updated quenching factor model
- ✓ Flux uncertainty now dominates the systematic uncertainty.
- ✓ Overall systematic uncertainty reduced: 28% →13%



COHERENT, PRL 129, 081801 (2022)

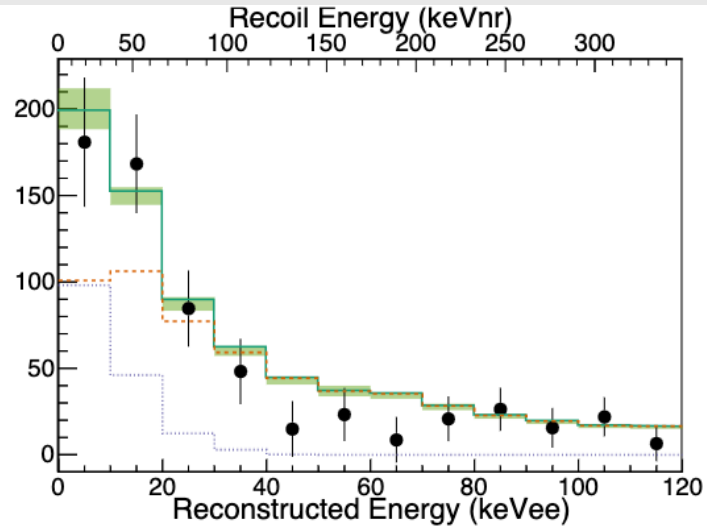
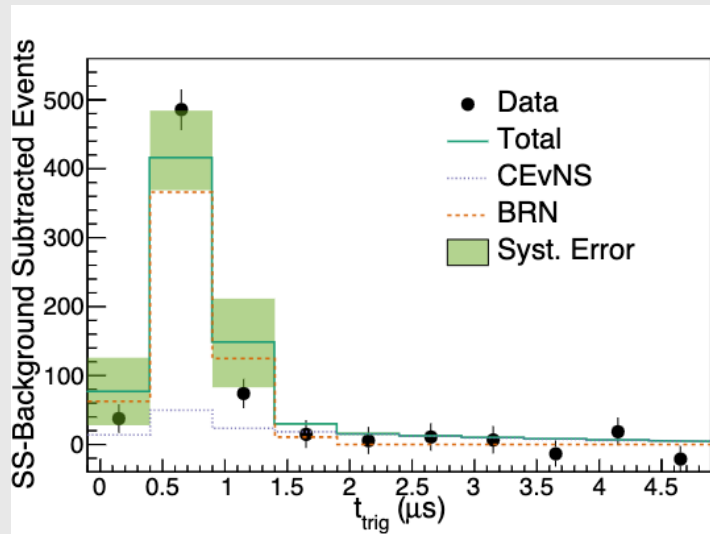
Leading actor II



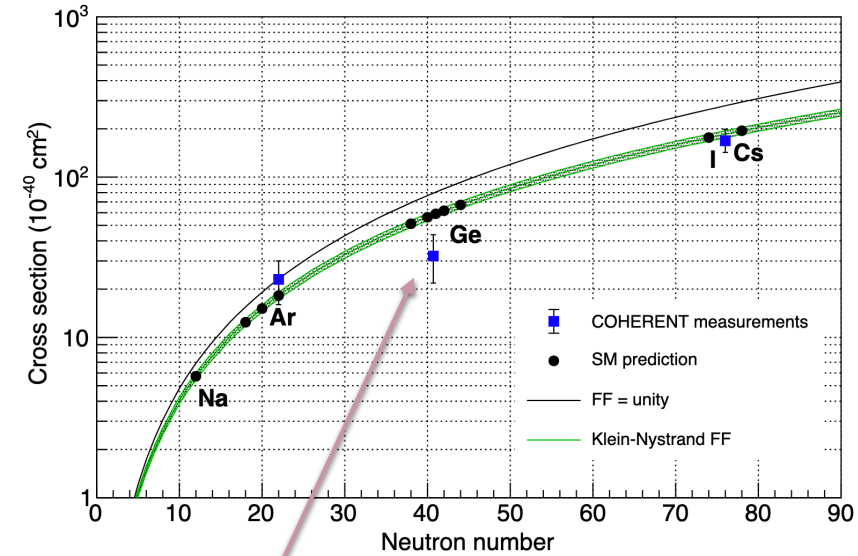
See D. Pershey talk

- 2020 first results using Ar, aka CENNS-10.
- Active mass of 24 kg of atmospheric argon
- Single phase only (scintillation), thr. ~ 20 keV_{nr}
- ✓ Two independent analyses observed a more than 3σ excess over background
- ✓ Still collecting data, more precise results expected soon.

COHERENT, PRL 126, 012002 (2021)



Verify the **expected neutron-number dependence** of cross-section



New COHERENT measurement on Ge crystals [arXiv:2406.13806]



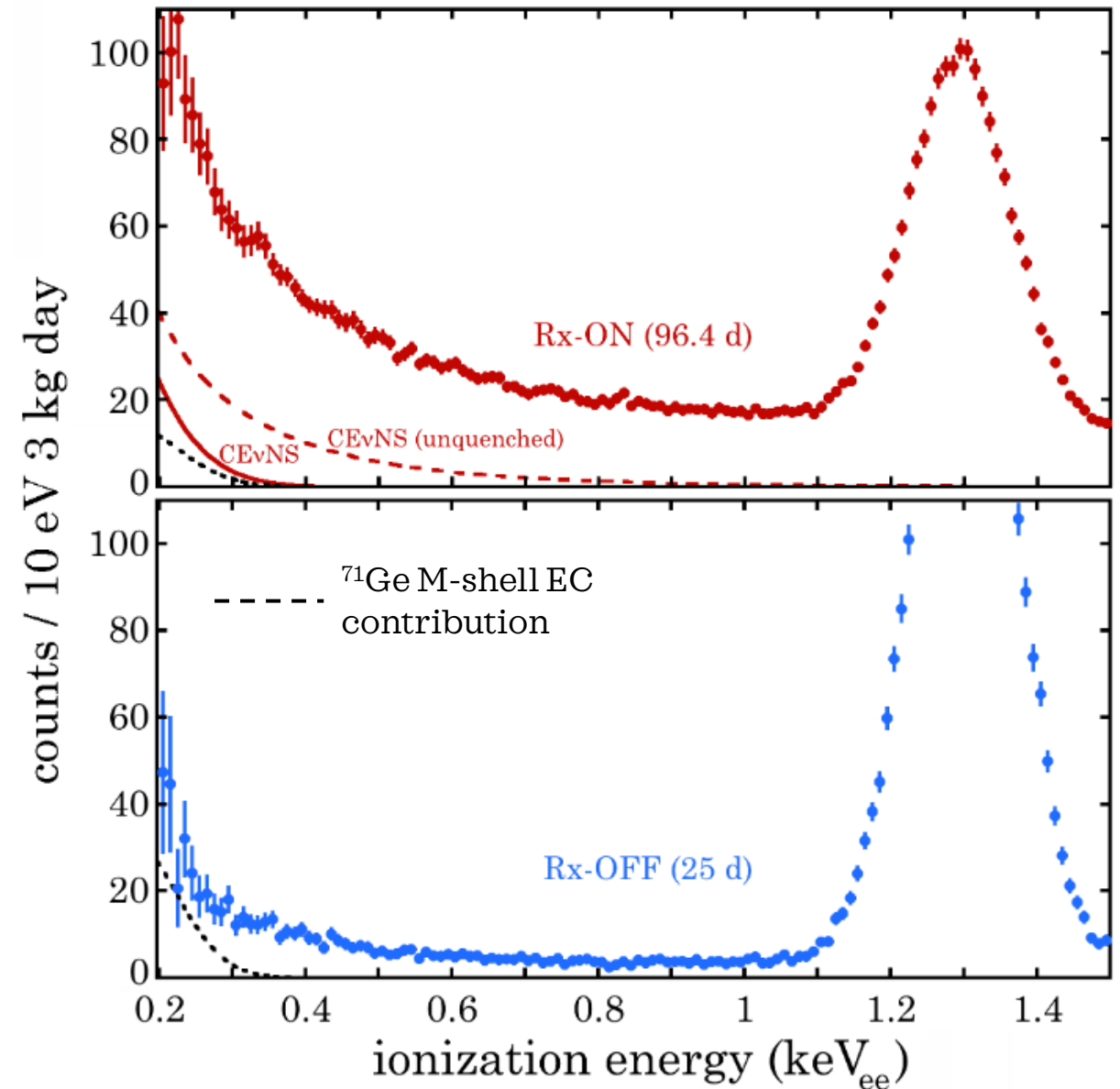
- CEvNS evidence at 3.9σ
- In agreement with the SM at 2σ

R. Bouabid (COHERENT) @Magnificent CEvNS 2024

Leading actor III



- 96.4 day (**Rx-ON**) exposure of a 3 kg ultra-low noise germanium detector (NCC-1701)
 - 10.39 m away from the Dresden-II boiling water reactor (P=2.96GW_{th})
 - **Low energy threshold:** 0.2 keV_{ee}
 - 25 days of reactor off (**Rx-OFF**)
 - The background comes from the elastic scattering of **epithermal neutrons** and the **electron capture in ⁷¹Ge**
- $$\frac{dN^{\text{bkg}}}{dT_e} = \underbrace{N_{\text{epith}} + A_{\text{epith}} e^{-T_e/T_{\text{epith}}}}_{\text{epithermal neutrons}} + \underbrace{\sum_{i=L1,L2,M} \frac{A_i}{\sqrt{2\pi}\sigma_i} e^{-\frac{(T_e-T_i)^2}{2\sigma_i^2}}}_{\text{electron capture in } ^{71}\text{Ge}}$$
- **Strong preference** (p<1.2x10⁻³) for the presence of CEνNS is found, when compared to a background-only model.



Many other results in the pipeline or expected soon...

- SNS neutrino flux uncertainty reduction from 10% to 2-3% in 5 years thanks to D₂O at the neutrino alley, upgrade of the SNS (higher beam power and energy)
- **NaIvETe**: CE ν NS on lighter nucleus Na, **COH-Ar-10** with 3 times more statistics and **CO-Ar-750** (ton scale), **COH-CryoCsI** with a significantly lower threshold (~ 0.5 KeVnr), ...



Plethora of other experiments expecting to detect CE ν NS soon!

E.g.: CONUS(+), NUCLEUS, MINER, ν GEN, RED-100, CONNIE, RICOCHE, NEON, CE ν NS @ ESS, Dark Matter experiments...

Soon, we can not afford to be sloppy anymore since we will reach the precision frontier!

Let's have a closer look ...

For more physics
with CEνNS look at
M. Cadeddu's talk

$$\frac{d\sigma^{CE\nu NS}(E_\nu, T_{nr})}{dT_{nr}} \cong \frac{G_F^2 m_N}{\pi} \left(1 - \frac{m_N T_{nr}}{2E_\nu^2}\right) \left[g_V^p(\sin^2(\vartheta_W)) Z F_Z(|\vec{q}|^2) + g_V^n N F_N(|\vec{q}|^2) \right]^2$$

Neutrino energy \rightarrow E_ν
 Mass of the nucleus \rightarrow m_N
 SM vector proton coupling \rightarrow g_V^p
 SM vector neutron coupling \rightarrow g_V^n
 Nuclear recoil energy \rightarrow T_{nr}
 Weinberg angle \rightarrow $\sin^2(\vartheta_W)$
 Proton Form Factor \rightarrow F_Z
 Neutron Form Factor \rightarrow F_N



At **tree-level** the CEνNS process is completely flavour-blind and the **SM vector couplings** are:

$$g_V^p(\nu_{e,\mu,\tau}) = \frac{1}{2} - 2\sin^2\vartheta_W \cong 0.0227$$

$$g_V^n(\nu_{e,\mu,\tau}) = -\frac{1}{2} = -0.5$$

Using $\sin^2\vartheta_W(q^2 \approx 0) = 0.23863(5)$

Radiative corrections for CE ν NS

When including the **UNIVERSAL radiative corrections** the couplings become:

$$g_V^p(\nu_\ell) = \rho \left(\frac{1}{2} - 2 \sin^2 \vartheta_W \right) + 2\boxtimes_{WW} + \square_{WW} - 2\phi_{\nu_\ell W} + \rho(2\boxtimes_{ZZ}^{uL} + \boxtimes_{ZZ}^{dL} - 2\boxtimes_{ZZ}^{uR} - \boxtimes_{ZZ}^{dR})$$

$$g_V^n = -\frac{\rho}{2} + 2\square_{WW} + \boxtimes_{WW} + \rho(2\boxtimes_{ZZ}^{dL} + \boxtimes_{ZZ}^{uL} - 2\boxtimes_{ZZ}^{dR} - \boxtimes_{ZZ}^{uR}).$$

Following the RGE formalism in Erler & Su, arXiv 1303.5522 (2013) as used in the PDG.

Where $\rho=1.00063$ represents a low-energy correction for neutral current processes and:

WW box $\square_{WW} = -\frac{\hat{\alpha}_Z}{2\pi\hat{s}_Z^2} \left[1 - \frac{\hat{\alpha}_s(M_W)}{2\pi} \right]$ **WW crossed-box** $\boxtimes_{WW} = \frac{\hat{\alpha}_Z}{8\pi\hat{s}_Z^2} \left[1 + \frac{\hat{\alpha}_s(M_W)}{\pi} \right]$

$\boxtimes_{ZZ}^{fX} = -\frac{3\hat{\alpha}_Z}{8\pi\hat{s}_Z^2\hat{c}_Z^2} (g_{LX}^{\nu_\ell f})^2 \left[1 - \frac{\hat{\alpha}_s(M_Z)}{\pi} \right]$ **ZZ box**

while the remaining **radiative term** is related to the so-called **neutrino charge radius**

$$\phi_{\nu_\ell W} = -\frac{\alpha}{6\pi} \left(\ln \frac{M_W^2}{m_\ell^2} + \frac{3}{2} \right)$$

Up to 67% difference wrt tree-level

In this scenario, **the couplings become flavour-dependent and different from tree-level:**

$$g_V^p(\nu_e) \simeq 0.0381$$

$$g_V^p(\nu_\mu) \simeq 0.0299$$

$$g_V^p(\nu_\tau) \simeq 0.0255$$

$$g_V^n \simeq -0.5117$$

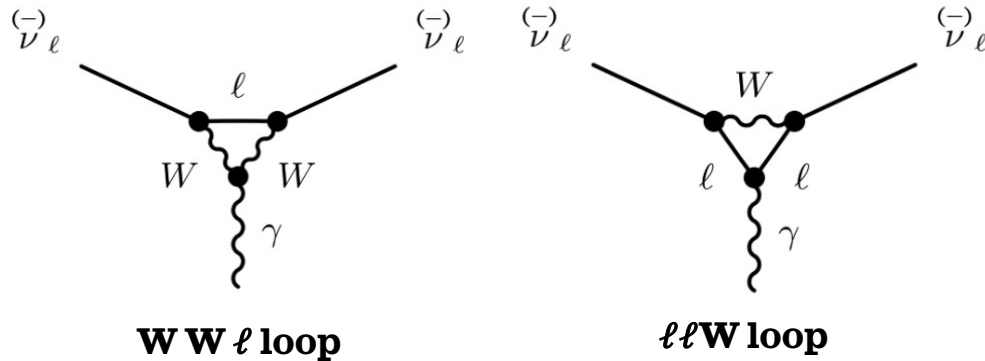


A hand holding a magnifying glass over a city street at night, with bokeh lights in the background. The magnifying glass focuses on a brightly lit street scene with many colorful signs and buildings. The background is filled with out-of-focus, colorful bokeh lights in shades of yellow, orange, blue, and pink.

NEUTRINO CHARGE RADIUS

Neutrino charge radius - definition

- The ν charge radius (NCR) **is a physical observable**, being finite and gauge invariant!
- The NCR is generated by **a loop insertion in the ν_ℓ line**, where W bosons and charged leptons ℓ **couple ν_ℓ with γ**
- In the SM, NCR is the **only electromagnetic property of neutrinos that is $\neq 0$** .



$$\langle r_{\nu_\ell}^2 \rangle_{\text{SM}} = -\frac{G_F}{2\sqrt{2}\pi^2} \left[\underset{\text{WW}\ell \text{ loop}}{3} - 2 \ln \left(\frac{m_\ell^2}{m_W^2} \right) \right]$$

Bernabeu et al, Phys.Rev.D62:113012 (2000)

$$\begin{aligned} \langle r_{\nu_e}^2 \rangle &\simeq -8.3 \times 10^{-33} \text{ cm}^2 \\ \langle r_{\nu_\mu}^2 \rangle &\simeq -4.8 \times 10^{-33} \text{ cm}^2 \\ \langle r_{\nu_\tau}^2 \rangle &\simeq -3.0 \times 10^{-33} \text{ cm}^2 \end{aligned}$$

The $\ell\ell W$ loop introduces a **dependence of the neutrino CR from the lepton flavour!**

- A neutral particle can be seen as the superposition of two charge distributions of opposite signs described by a **charge form factor** which is nonzero only for momentum transfers $q^2 \neq 0$

$$f_Q(q^2) = \cancel{f_Q(0)} + q^2 \frac{df_Q(q^2)}{dq^2} \Big|_{q^2=0} + \dots$$

=0 since ν s are neutral

$$\langle r^2 \rangle \equiv 6 \frac{df_Q(q^2)}{dq^2} \Big|_{q^2=0}$$

Neutrino charge radius definition
i.e. the radius of the electric charge distribution

Neutrino charge radius – practically speaking

- The neutrino CR affects the scattering of neutrinos with charged particles.
- In the case of CEvNS, **it contributes only to the NC proton coupling and enters in the radiative correction**

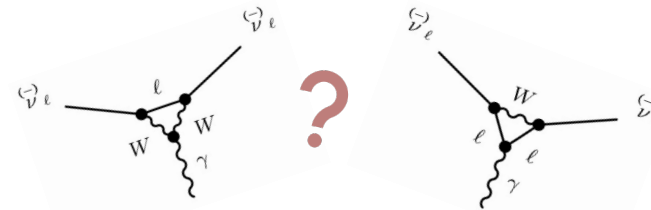
CEvNS case: $g_V^p \rightarrow \tilde{g}_V^p - \frac{2}{3} M_W^2 \langle r_{\nu_\ell}^2 \rangle \sin^2 \vartheta_W \rightarrow \sin^2 \vartheta_W \left(1 + \frac{1}{3} M_W^2 \langle r_{\nu_\ell}^2 \rangle \right)$

$\simeq 0.0184$ EW proton coupling without the contribution of the SM charge radius

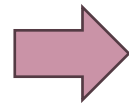
It can be seen as an effective shift of the weak mixing angle

Not fixing the NCR value to SM in the radiative correction: interesting quantity to measure!

- So far, **only constraints** have been put on its value.
- **New particles entering the loops could modify it**



- However, keep in mind that the neutrino charge radius is defined at $q^2 \equiv 0$, while **none of the experiments is performed at null-momentum transfer!**



Must be taken into account when implementing radiative corrections in CEvNS processes and when measuring the ν charge radius!

How to deal with non-null momentum transfers?

- Look at **process - dependent radiative corrections** defined by Marciano et al. in arXiv:0403168.

$$\sin^2 \vartheta_W(q^2) = k_{\nu_\ell}(q^2) \sin^2 \vartheta_W(M_Z) \leftarrow \text{They are hidden in wma running!}$$

where for **neutrino scattering**:

$$k_{\nu_\ell}(q^2) = 1 - \frac{\alpha}{2\pi\hat{s}_Z^2} \left[2 \sum_f (T_{3f} Q_f - 2\hat{s}_Z^2 Q_f^2) J_f(q^2) + \frac{\hat{c}_Z^2}{3} + \frac{1}{\hat{c}_Z^2} \left(\frac{19}{8} + \frac{17}{4} \hat{s}_Z^2 + 3\hat{s}_Z^4 \right) \right. \\ \left. - \left(\frac{7}{2} \hat{c}_Z^2 + \frac{1}{12} \right) \ln \hat{c}_Z^2 \right] \boxed{-\frac{\alpha}{\pi\hat{s}_Z^2} \left[-R_\ell(q^2) + \frac{1}{4} \right]}, \quad \text{with:} \\ R_\ell(0) = \frac{1}{6} \ln \frac{m_\ell^2}{M_W^2} \\ R_\ell(q^2) = \int_0^1 dx x(1-x) \ln \left[\frac{m_\ell^2 - q^2 x(1-x)}{M_W^2} \right]$$

For $q^2 \rightarrow 0$ the radiative correction in the two formalisms agree:

$$\boxed{\phi_{\nu_\ell W} = -\frac{\alpha}{\pi} \left(-R_\ell(0) + \frac{1}{4} \right)} \longleftrightarrow \boxed{\phi_{\nu_\ell W} = -\frac{\alpha}{6\pi} \left(\ln \frac{M_W^2}{m_\ell^2} + \frac{3}{2} \right)}$$

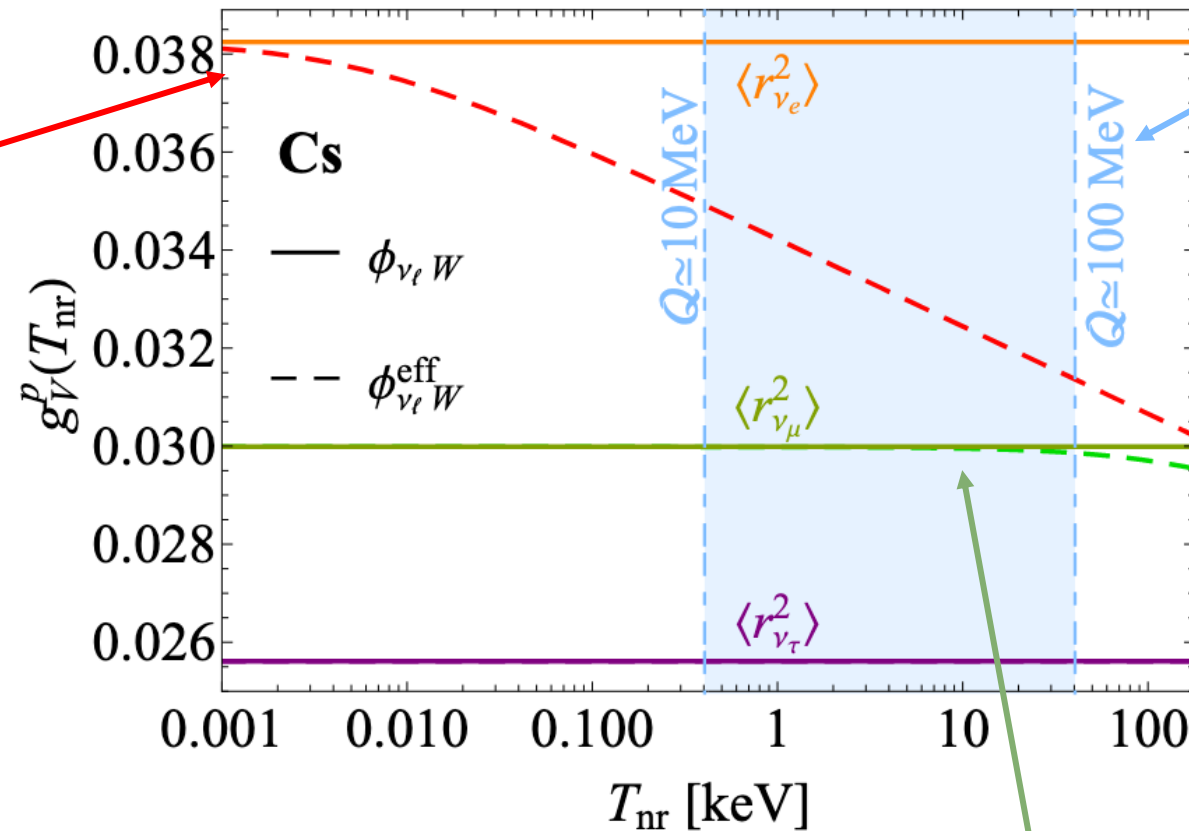
with a **clear advantage**:

$$\phi_{\nu_\ell W}^{\text{eff}}(q^2) = -\frac{\alpha}{\pi} \left(-\underbrace{R_\ell(q^2)}_{\text{circled}} + \frac{1}{4} \right) \quad \text{This CR effective radiative correction includes the } q^2 \text{ dependence!}$$

Effects on the vector proton coupling

Considering the **neutrino CR radiative correction inside the EW proton coupling**: **impact visible for $q^2 \gtrsim m_\ell^2$**

For ν_e processes: the correction becomes visible for $q \gtrsim 0.5$ MeV



E.g. COHERENT probes $Q \sim 10 - 100$ MeV

10-20% difference in the ν_e proton coupling!

↓

~1% effect on the ν_e -N cross section

↓

~0.5% effect on the total Cs CEvNS rate

* $Q^2 = -q^2 \simeq 2m_{\text{tar}}T$

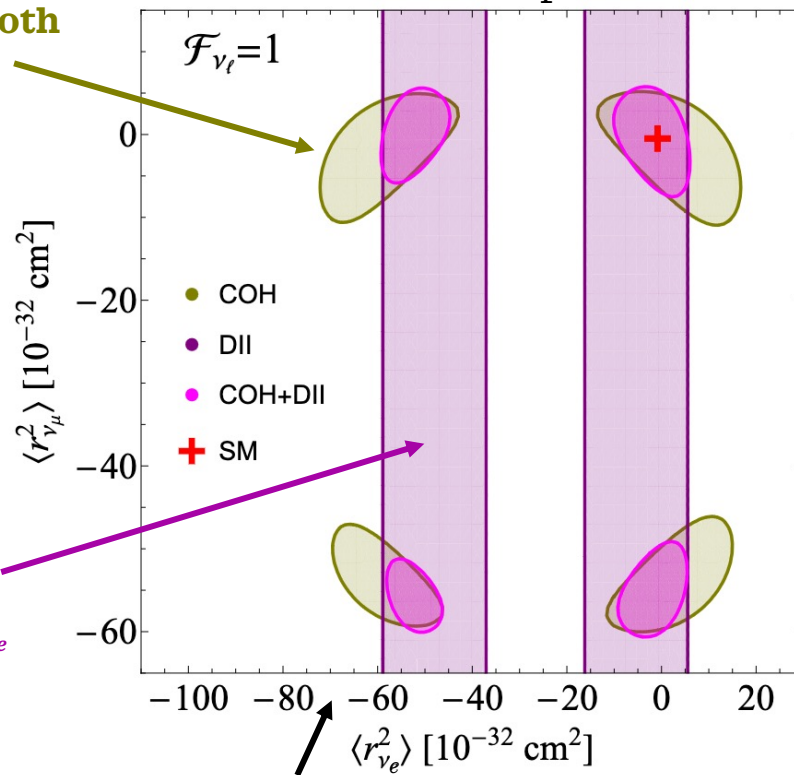
For ν_μ processes visible only for $q \gtrsim 100$ MeV

Neutrino charge radius constraints

We introduce a **neutrino charge-radius form factor**: $\mathcal{F}_{\nu_\ell}(T_{\text{nr}}) = \frac{\langle r_{\nu_\ell}^2 \rangle^{\text{eff}}(T_{\text{nr}})}{\langle r_{\nu_\ell}^2 \rangle^{\text{eff}}(0)} \equiv \frac{\langle r_{\nu_\ell}^2 \rangle^{\text{eff}}(T_{\text{nr}})}{\langle r_{\nu_\ell}^2 \rangle^{\text{SM}}} \xrightarrow{q \rightarrow 0} \mathcal{F}_{\nu_\ell}(T_{\text{nr}}) = 1$

COHERENT is sensitive to both $r_{\nu_e}^2$ and $r_{\nu_\mu}^2$

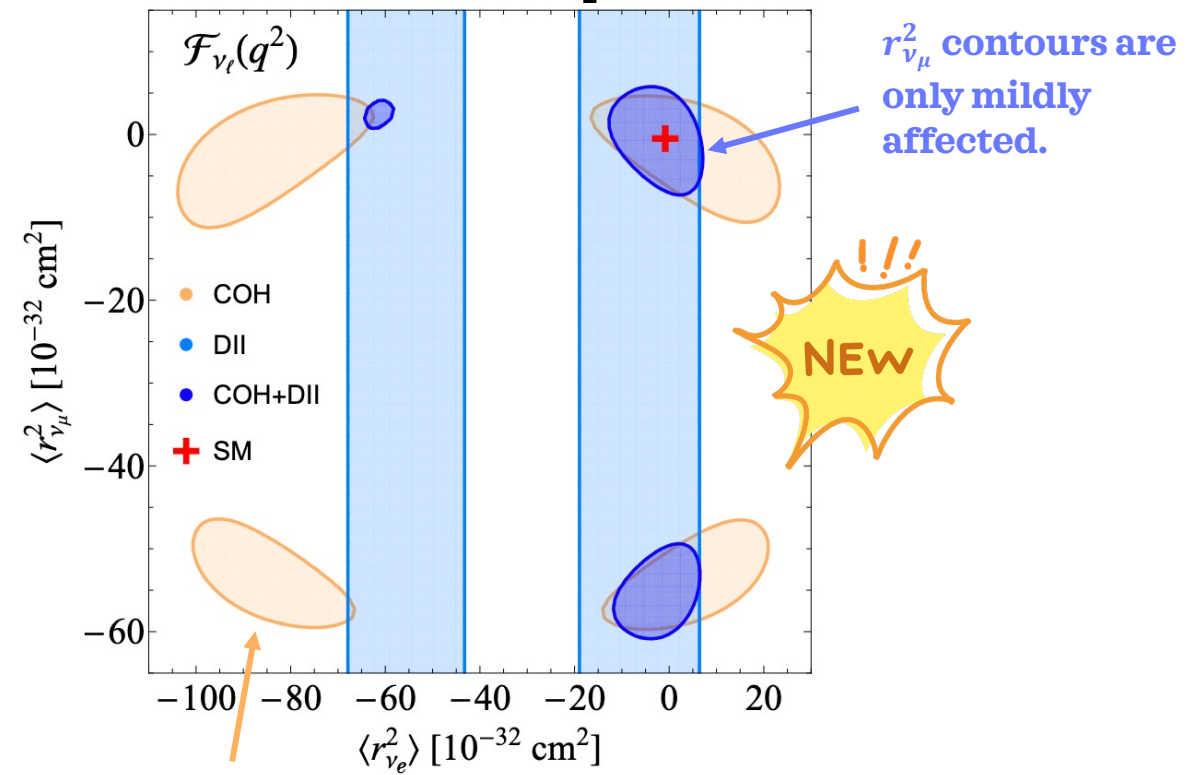
No-momentum dependence



Bands since reactors exp. are only sensitive to $r_{\nu_e}^2$

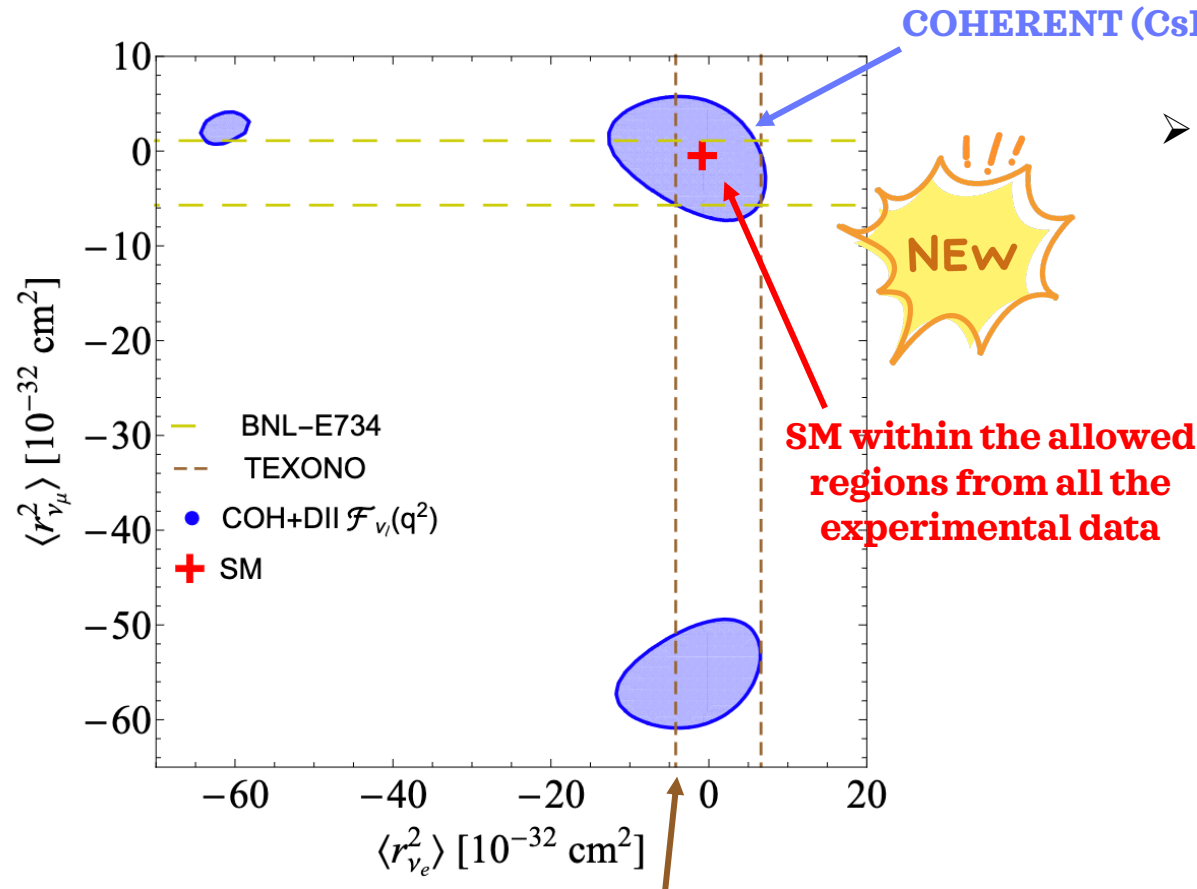
These largely negative values are due to degenerate cross-section

With momentum dependence



COHERENT Ar + CsI $r_{\nu_e}^2$ results are more affected than reactors due to the larger momentum transfer

Neutrino charge radius combined results



- The main impact of accounting for the neutrino CR form factor is that, by combining the different CEvNS measurements, the **allowed regions in the parameter space are significantly reduced!**

At 90% CL:

Best upper limit!

$$-9.5 < \langle r_{\nu_e}^2 \rangle [10^{-32} \text{ cm}^2] < 5.5,$$

$$-59.2 < \langle r_{\nu_\mu}^2 \rangle [10^{-32} \text{ cm}^2] < -51.0,$$

$$-5.9 < \langle r_{\nu_\mu}^2 \rangle [10^{-32} \text{ cm}^2] < 4.1.$$

+ Large $r_{\nu_e}^2$ negative values almost excluded!

Current best limits from accelerator $\nu_{e/\mu} - e$ scattering

also shown: **TEXONO** $-4.2 < \langle r_{\nu_e}^2 \rangle < 6.6 [10^{-32} \text{ cm}^2]$,

BNL-E734 $-5.7 < \langle r_{\nu_\mu}^2 \rangle < 1.1 [10^{-32} \text{ cm}^2]$ @90% CL



Conclusions

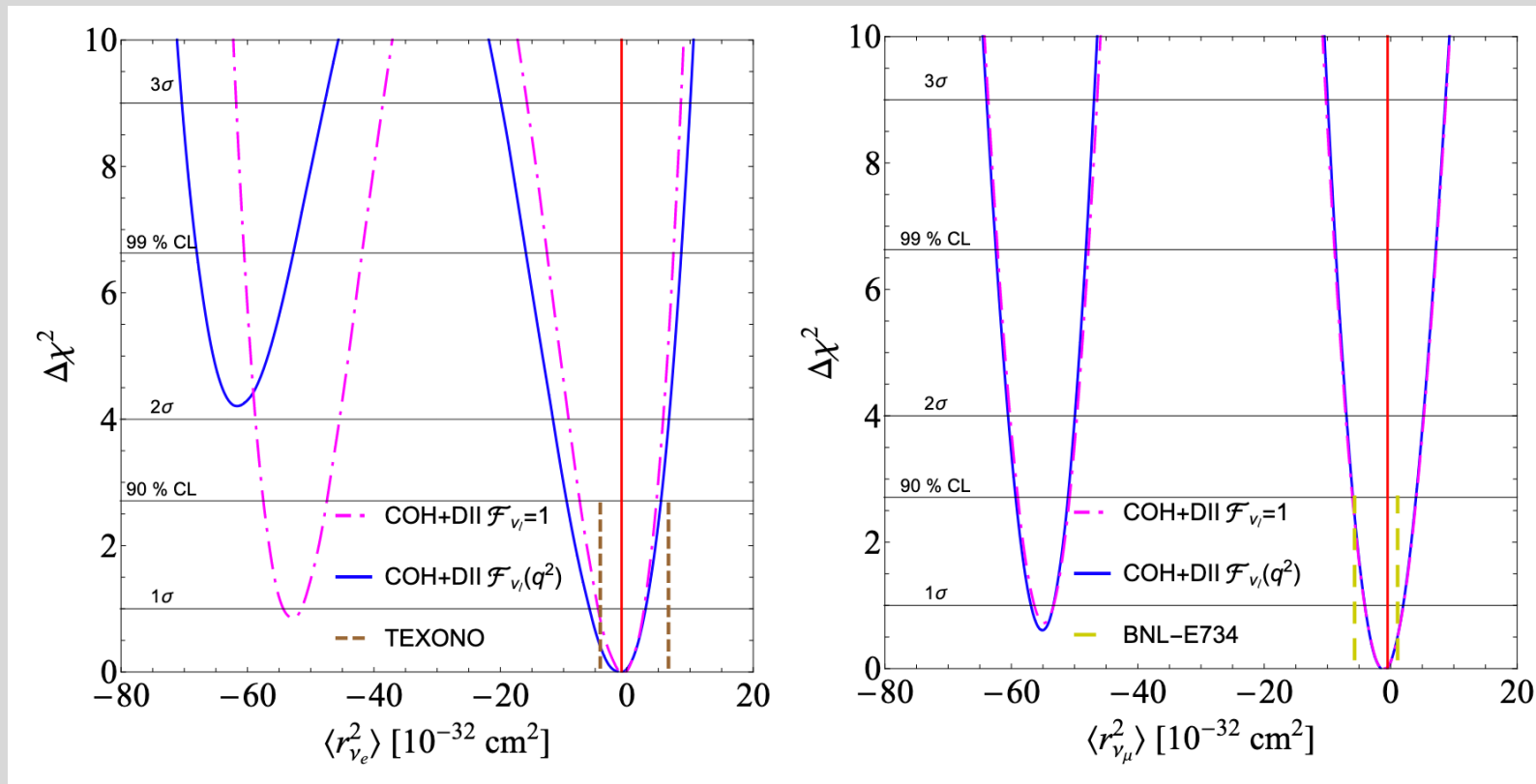
- **Radiative corrections cannot be neglected!**
- Need to **properly account for the non-null momentum transfer of the experiments** in the calculation of the neutrino charge radius radiative correction.
- The systematic bias of the $\nu_e N$ scattering cross section is around 1 -2%, which is an **effect of ~20% with respect to the current systematic uncertainties** affecting CEvNS.
- **Mandatory to consider it to extract unbiased charge radii:** moreover it restricts the available phase space.

For future high precision measurements, it will become imperative to include the momentum dependence!



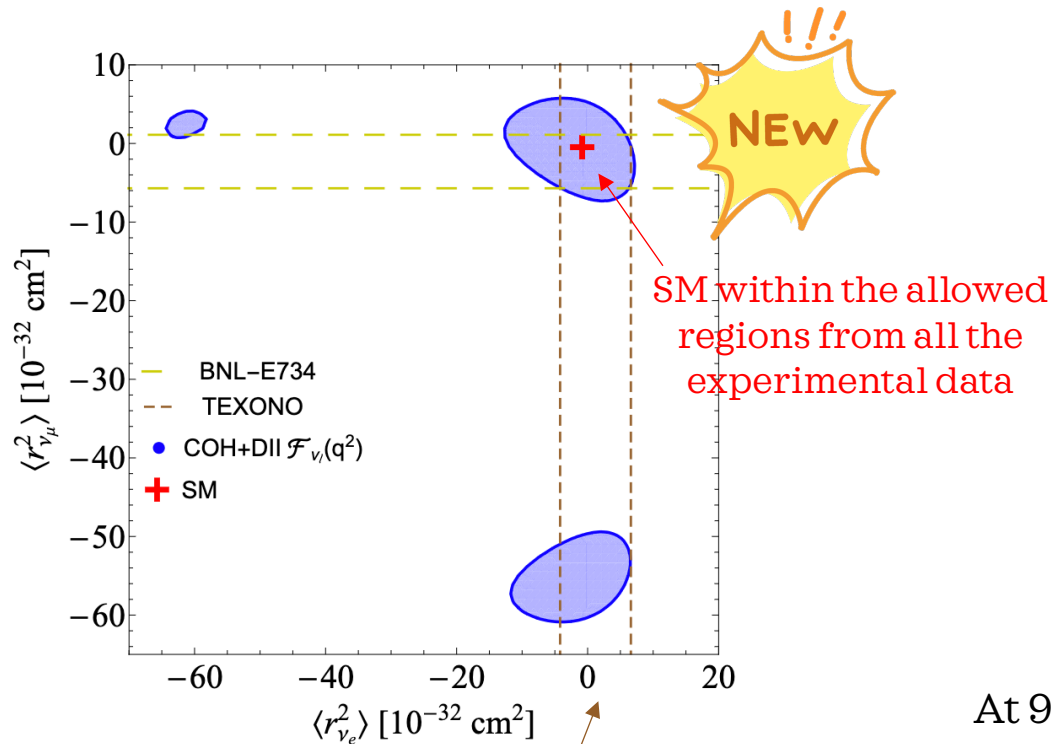
BACKUP

1D PROJECTIONS



Results – A global view

- The main impact of accounting for the neutrino CR form factor is that, by combining the different measurements, the **allowed regions in the parameter space are significantly reduced!**



Current best limits from accelerator $\nu_{e/\mu} - e$ scattering also shown: **TEXONO** $-4.2 < \langle r_{\nu_e}^2 \rangle < 6.6 [10^{-32} \text{ cm}^2]$, **BNL-E734** $-5.7 < \langle r_{\nu_\mu}^2 \rangle < 1.1 [10^{-32} \text{ cm}^2]$ @90% CL

| | 1σ | 90% | 2σ | 3σ |
|---------------------------------------|--------------------------------|---------------------------------|----------------------------------|---------------------------------|
| COHERENT (CsI+Ar) | | | | |
| $\langle r_{\nu_e}^2 \rangle$ | (-95.0, -77.4) (0.09, 12.8) | (-100.0, -69.8) (-8.6, 19.1) | (-102.6, -64.8) (-13.9, 22.2) | (-110.4, 30.7) |
| $\langle r_{\nu_\mu}^2 \rangle$ | (-6.8, 0.5) | (-57.6, -48.9) (-9.3, 2.9) | (-59.2, -47.1) (-10.7, 4.2) | (-63.3, -42.3) (-15.2, 8.1) |
| Dresden-II | | | | |
| $\langle r_{\nu_e}^2 \rangle$ | (-62.5, -53.7) (-9.0, 1.8) | (-65.7, -48.5) (-13.8, 4.5) | (-67.2, -45.0) (-17.2, 6.0) | (-71.1, 9.7) |
| COHERENT (CsI+Ar) + Dresden-II | | | | |
| $\langle r_{\nu_e}^2 \rangle$ | (-5.8, 3.1) | (-9.5, 5.5) | (-11.6, 6.8) | (-70.3, -47.7) (-19.8, 10.1) |
| $\langle r_{\nu_\mu}^2 \rangle$ | (-56.8, -53.3) (-4.0, 2.1) | (-59.2, -51.0) (-5.9, 4.1) | (-60.4, -49.9) (-6.9, 5.3) | (-63.8, -46.8) (-9.9, 8.7) |

At 90% CL:

$$-9.5 < \langle r_{\nu_e}^2 \rangle [10^{-32} \text{ cm}^2] < 5.5, \quad \text{Best upper limit!}$$

$$-59.2 < \langle r_{\nu_\mu}^2 \rangle [10^{-32} \text{ cm}^2] < -51.0, \quad -5.9 < \langle r_{\nu_\mu}^2 \rangle [10^{-32} \text{ cm}^2] < 4.1$$

Agreement between the two formalisms

It can be noticed that the difference of the weak mixing angle values consists only of a small constant term:

$$k_{\nu_\ell}(q^2 = 0)\hat{s}_Z^2 - \hat{s}_0^2(\text{RGE}) = -\frac{2\alpha}{9\pi} + \mathcal{O}(\alpha^2)$$

See also Appendix A of arXiv: 2309.04060

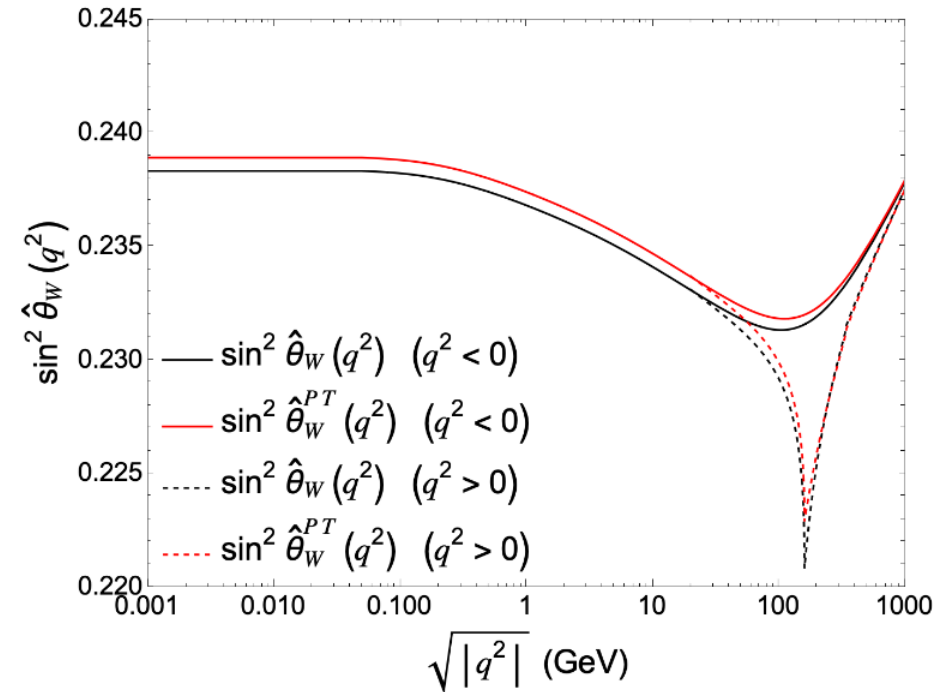
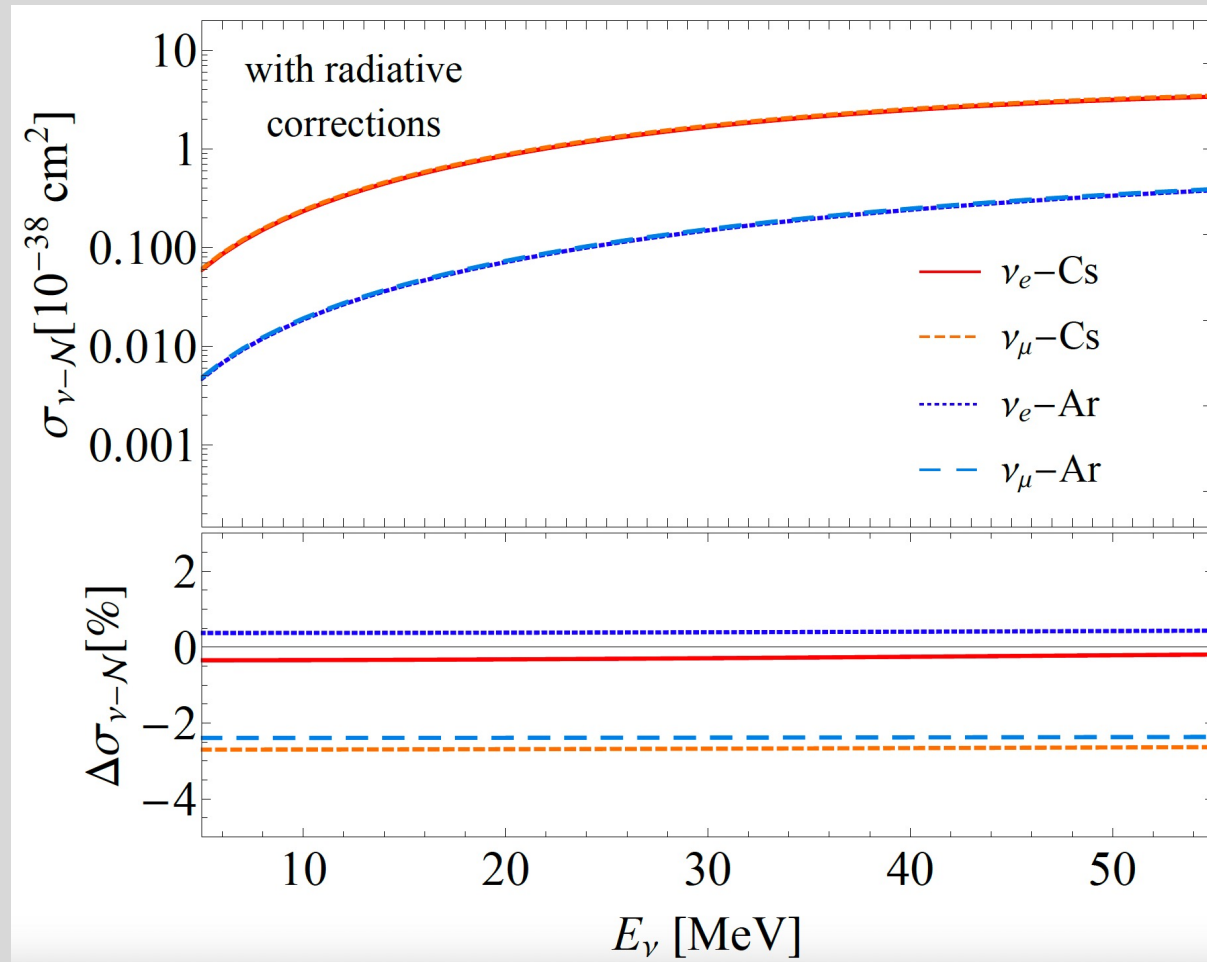


FIG. 9. A comparison of typical form $\sin^2 \hat{\theta}_W(q^2)$ in black and PT form $\sin^2 \hat{\theta}_W^{PT}(q^2)$ in red. Solid (dashed) curves represent spacelike (timelike) momenta. The curves for timelike momenta are shown only in a domain $\sqrt{|q^2|} > 20$ GeV.

Impact of radiative corrections @ $q^2=0$



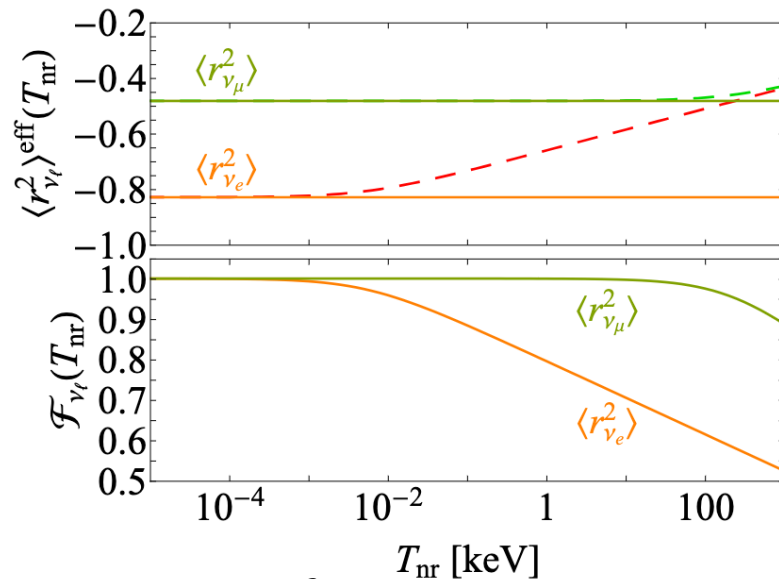
From N. Cargioli PhD's thesis

The effective charge radius form factor

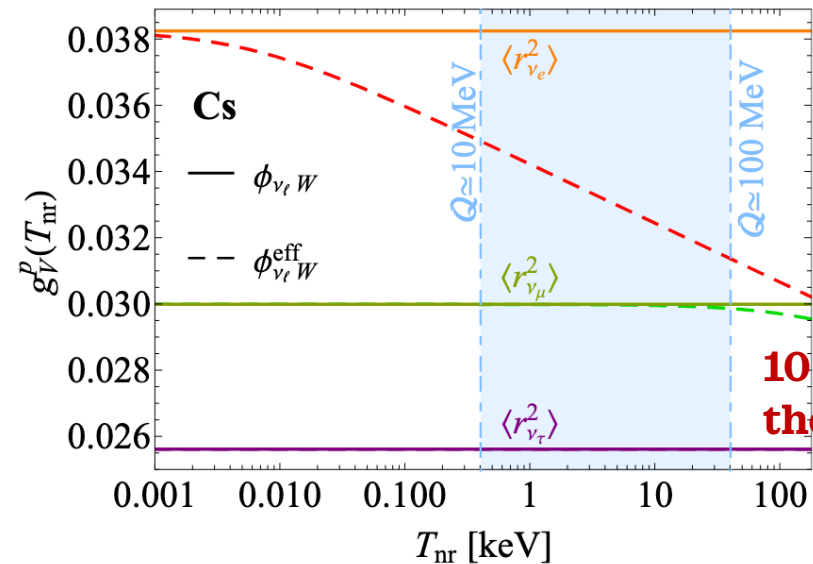
We introduce a **neutrino charge radius form factor** $\mathcal{F}_{\nu_\ell}(T_{\text{nr}}) = \frac{\langle r_{\nu_\ell}^2 \rangle^{\text{eff}}(T_{\text{nr}})}{\langle r_{\nu_\ell}^2 \rangle^{\text{eff}}(0)} \equiv \frac{\langle r_{\nu_\ell}^2 \rangle^{\text{eff}}(T_{\text{nr}})}{\langle r_{\nu_\ell}^2 \rangle^{\text{SM}}}$

with $\langle r_{\nu_\ell}^2 \rangle^{\text{eff}} = \frac{6G_F}{\sqrt{2}\pi\alpha} \phi_{\nu_\ell W}^{\text{eff}}(q^2) = -\frac{G_F}{2\sqrt{2}\pi^2} [3 - 12R_\ell(q^2)]$

From which we obtain an updated proton coupling:



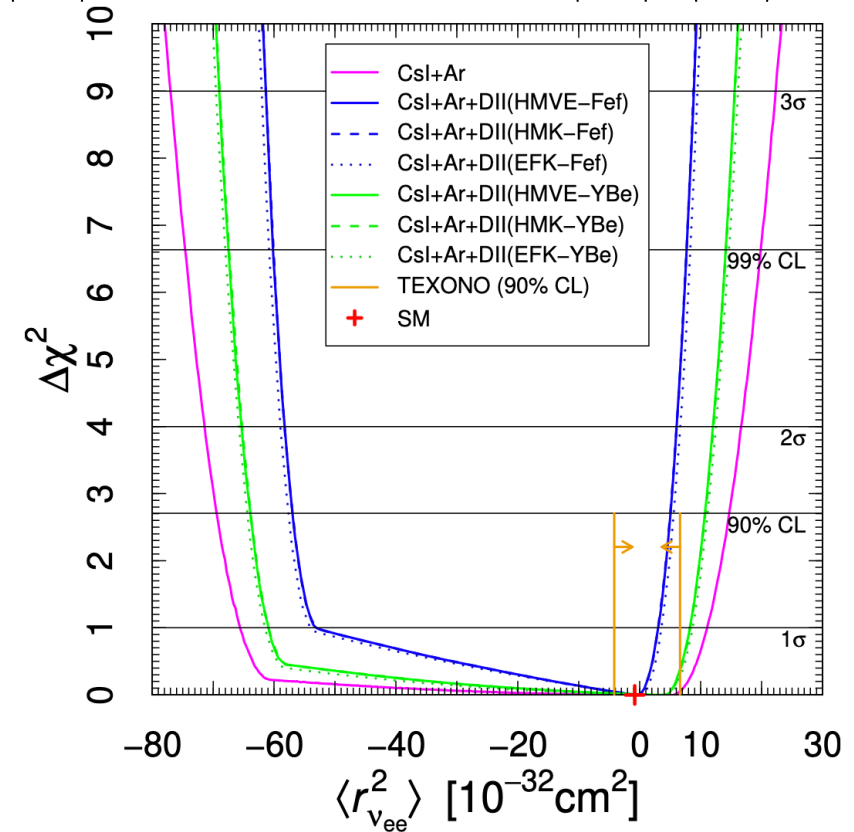
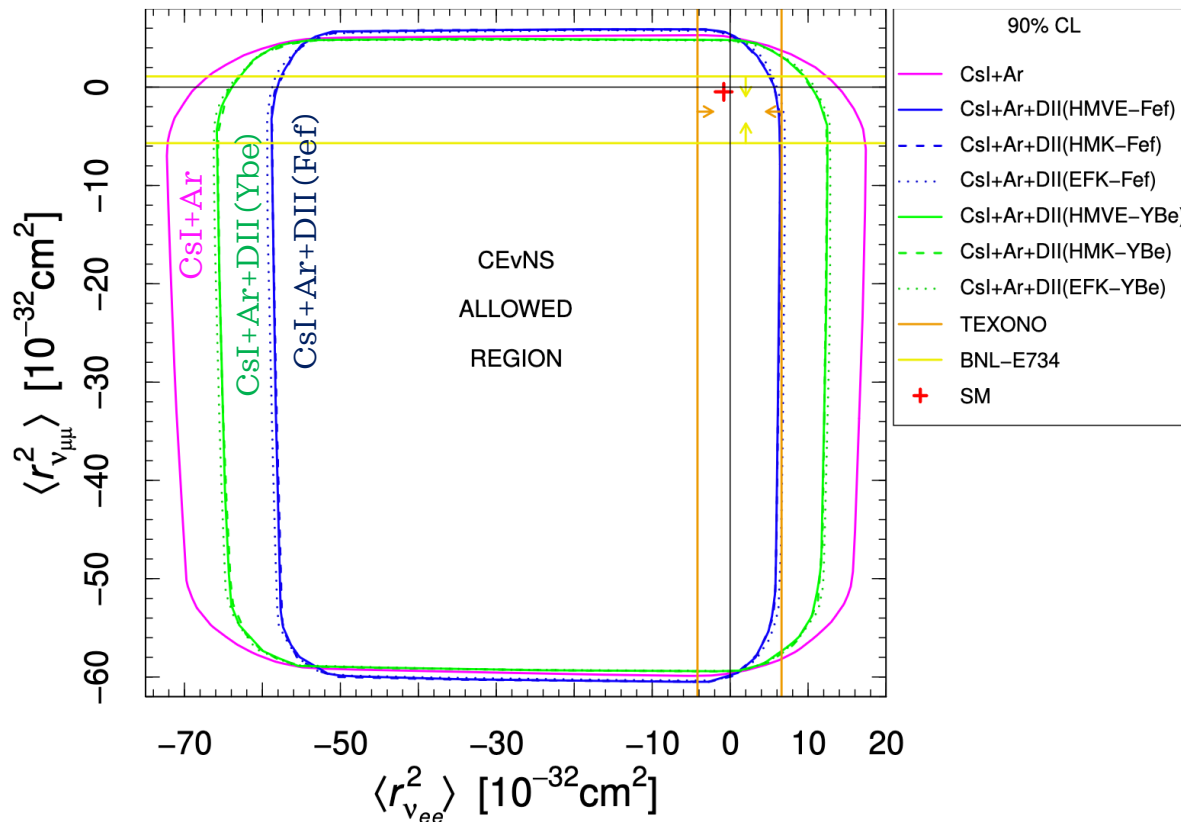
Impact visible for $q^2 \gtrsim m_\ell^2$, for ν_e processes the correction to the couplings becomes visible for $q \gtrsim 0.5$ MeV, while for ν_μ only above ~ 100 MeV!



10-20% difference in the proton coupling!

Neutrino charge radius – previous results

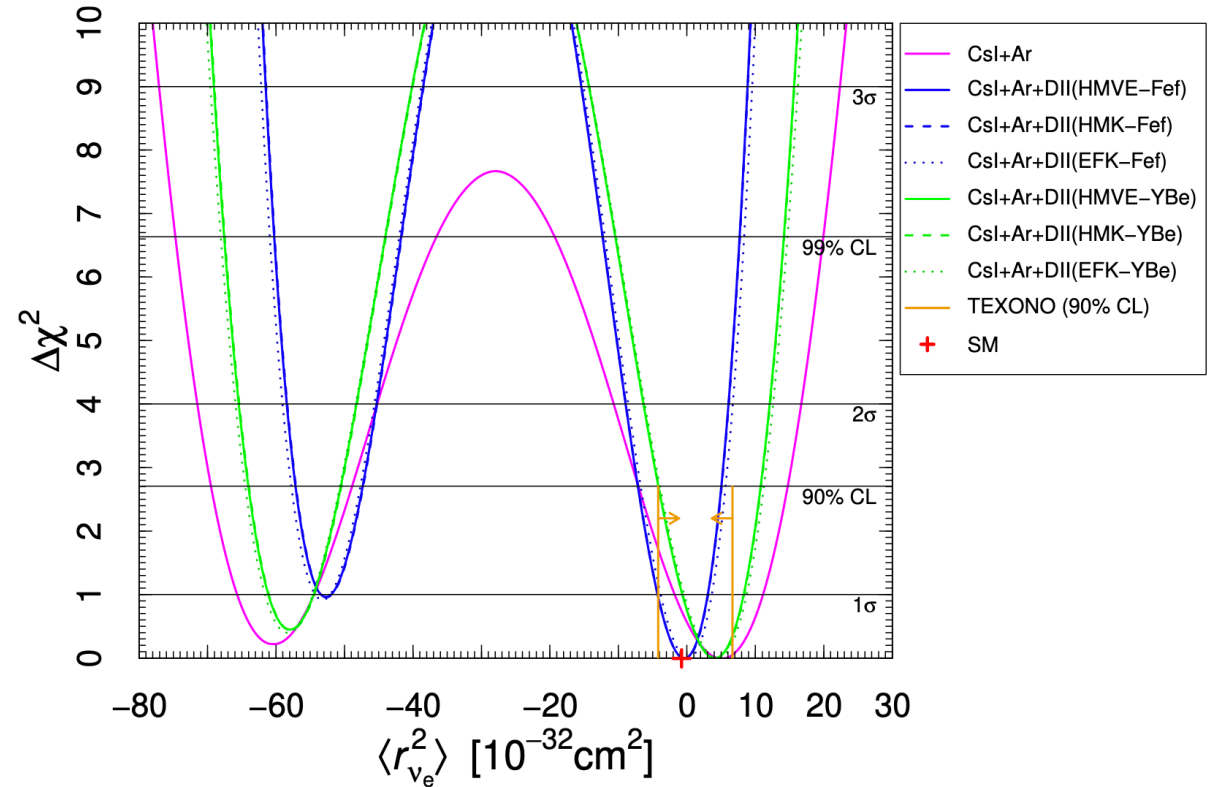
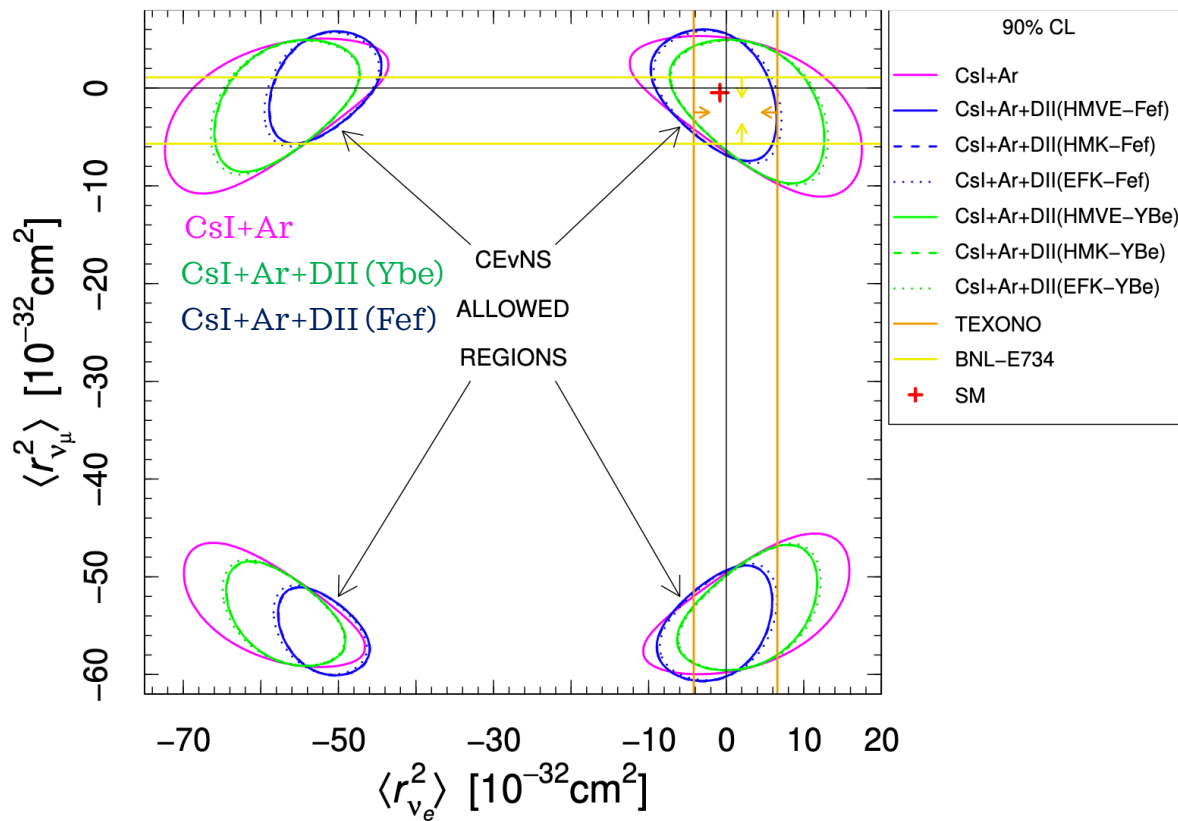
Assuming the **presence of transition CR**, **DRESDEN-II** can measure $\langle r_{\nu_{ee}}^2 \rangle, |\langle r_{\nu_{e\mu}}^2 \rangle|, |\langle r_{\nu_{e\tau}}^2 \rangle|$ **COHERENT** also $|\langle r_{\nu_{\mu\tau}}^2 \rangle|, \langle r_{\nu_{\mu\mu}}^2 \rangle$



- The CsI + Ar COHERENT combination is **vastly dominated by CsI**.
- **Dresden-II** and **CsI** datasets contribute with **roughly same precision**.
- **HMVE, HMK, EFK** different flux parametrization: practically independent, **highly sensitive to the QF used**.

Neutrino charge radius – previous results

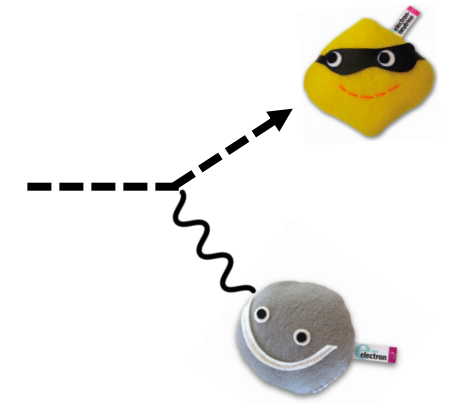
Assuming the **absence of transition CR**: $\langle r_{\nu_e}^2 \rangle \equiv \langle r_{\nu_{ee}}^2 \rangle$ and $\langle r_{\nu_\mu}^2 \rangle \equiv \langle r_{\nu_{\mu\mu}}^2 \rangle$



$-7.1 < \langle r_{\nu_e}^2 \rangle < 5 [10^{-32} \text{cm}^2]$ **COHERENT + DRESDEN-II @ 90% CL**

- When using the Fef QF we **set a better upper bound with respect to that set by TEXONO** ($6.6 \times 10^{-32} \text{cm}^2$)
- **No effect is found due to ES** on the neutrino CR, thus the results are independent of its inclusion

ELASTIC ν – ELECTRON SCATTERING



- ν -electron elastic scattering (ES) is a **concurrent process to CEvNS**
- In the SM, its contribution to the total event rate is small and can be neglected
- **In certain BSM scenarios the ES contribution increases significantly** ➔ Allows us to achieve stronger constraints !

Neutrino energy

Mass of the electron

SM neutrino electron coupling

$$\frac{d\sigma^{ES}(E_\nu, T_e)}{dT_e} = Z_{eff}^A(T_e) \frac{G_F^2 m_e}{2\pi} \left[(g_V^{\nu_l} + g_A^{\nu_l})^2 + (g_V^{\nu_l} - g_A^{\nu_l})^2 \left(1 - \frac{T_e}{E_\nu}\right)^2 - ((g_V^{\nu_l})^2 - (g_A^{\nu_l})^2) \frac{m_e T_e}{E_\nu^2} \right] + \text{radiative corrections}$$

Electron recoil energy

The interaction is not with free electrons but atomic electrons!
Quantifies the **number of electrons that can be ionized by a certain energy deposit T_e** .

- The $Z_{eff}^A(T_e)$ term is needed to correct the cross section derived under the Free Electron Approximation (FEA) hypothesis, where electrons are considered to be free and at rest (would just scale as Z).
 - Alternative ab-initio approach: **multi-configuration relativistic random phase approximation** (MCRRPA) able to improve the description of the atomic many-body effects
 - We do not include such contribution for Ar, where the f_{90} parameter removes electron recoils due to ES
- ☐ PRA 25 (1982) 634

The Z_{eff} term

| | | | | | |
|--------------------------------|--|---|--|-----|---|
| $Z_{\text{eff}}^{\text{Cs}} =$ | 55, | $T_e > 35.99 \text{ keV}$ | $Z_{\text{eff}}^{\text{I}} =$ | 53, | $T_e > 33.17 \text{ keV}$ |
| | 53, | $35.99 \text{ keV} \geq T_e > 5.71 \text{ keV}$ | | 51, | $33.17 \text{ keV} \geq T_e > 5.19 \text{ keV}$ |
| | 51, | $5.71 \text{ keV} \geq T_e > 5.36 \text{ keV}$ | | 49, | $5.19 \text{ keV} \geq T_e > 4.86 \text{ keV}$ |
| | 49, | $5.36 \text{ keV} \geq T_e > 5.01 \text{ keV}$ | | 47, | $4.86 \text{ keV} \geq T_e > 4.56 \text{ keV}$ |
| | 45, | $5.01 \text{ keV} \geq T_e > 1.21 \text{ keV}$ | | 43, | $4.56 \text{ keV} \geq T_e > 1.07 \text{ keV}$ |
| | 43, | $1.21 \text{ keV} \geq T_e > 1.07 \text{ keV}$ | | 41, | $1.07 \text{ keV} \geq T_e > 0.93 \text{ keV}$ |
| | 41, | $1.07 \text{ keV} \geq T_e > 1 \text{ keV}$ | | 39, | $0.93 \text{ keV} \geq T_e > 0.88 \text{ keV}$ |
| | 37, | $1 \text{ keV} \geq T_e > 0.74 \text{ keV}$ | | 35, | $0.88 \text{ keV} \geq T_e > 0.63 \text{ keV}$ |
| | 33, | $0.74 \text{ keV} \geq T_e > 0.73 \text{ keV}$ | | 31, | $0.63 \text{ keV} \geq T_e > 0.62 \text{ keV}$ |
| | 27, | $0.73 \text{ keV} \geq T_e > 0.23 \text{ keV}$ | | 25, | $0.62 \text{ keV} \geq T_e > 0.19 \text{ keV}$ |
| 25, | $0.23 \text{ keV} \geq T_e > 0.17 \text{ keV}$ | 23, | $0.19 \text{ keV} \geq T_e > 0.124 \text{ keV}$ | | |
| 23, | $0.17 \text{ keV} \geq T_e > 0.16 \text{ keV}$ | 21, | $0.124 \text{ keV} \geq T_e > 0.123 \text{ keV}$ | | |
| 19, | $T_e < 0.16 \text{ keV}$ | 17, | $T_e < 0.123 \text{ keV}$ | | |

Table 1. The effective electron charge of the target atom, $Z_{\text{eff}}^{\text{A}}(T_e)$, for Cs and I.

| | | |
|--------------------------------|-----|--|
| $Z_{\text{eff}}^{\text{Ge}} =$ | 32, | $T_e > 11.103 \text{ keV}$ |
| | 30, | $11.103 \text{ keV} \geq T_e > 1.4146 \text{ keV}$ |
| | 28, | $1.4146 \text{ keV} \geq T_e > 1.2481 \text{ keV}$ |
| | 26, | $1.2481 \text{ keV} \geq T_e > 1.217 \text{ keV}$ |
| | 22, | $1.217 \text{ keV} \geq T_e > 0.1801 \text{ keV}$ |
| | 20, | $0.1801 \text{ keV} \geq T_e > 0.1249 \text{ keV}$ |
| | 18, | $0.1249 \text{ keV} \geq T_e > 0.1208 \text{ keV}$ |
| | 14, | $0.1208 \text{ keV} \geq T_e > 0.0298 \text{ keV}$ |
| | 10, | $0.0298 \text{ keV} \geq T_e > 0.0292 \text{ keV}$ |
| | 4, | $T_e \leq 0.0292 \text{ keV}$ |

Table 2. The effective electron charge of the target atom, $Z_{\text{eff}}^{\text{A}}(T_e)$, for Ge.

Specific for each atom, obtained using edge energies from photo-absorption data.

 A. Thompson et al., X-ray data booklet, <https://xdb.lbl.gov/>, Lawrence Berkeley National Laboratory, U.S.A. (2009)

The charge radii summary

| Process | Collaboration | Limit [10^{-32} cm ²] | C.L. | Ref. |
|---|-------------------|---|------|------------------------|
| Reactor $\bar{\nu}_e$ - e | Krasnoyarsk | $ \langle r_{\nu_e}^2 \rangle < 7.3$ | 90% | [94] |
| | TEXONO | $-4.2 < \langle r_{\nu_e}^2 \rangle < 6.6$ | 90% | [91] ^a |
| Accelerator ν_e - e | LAMPF | $-7.12 < \langle r_{\nu_e}^2 \rangle < 10.88$ | 90% | [95] ^a |
| | LSND | $-5.94 < \langle r_{\nu_e}^2 \rangle < 8.28$ | 90% | [96] ^a |
| Accelerator ν_μ - e and $\bar{\nu}_\mu$ - e | BNL-E734 | $-5.7 < \langle r_{\nu_\mu}^2 \rangle < 1.1$ | 90% | [92] ^{a, b} |
| | CHARM-II | $ \langle r_{\nu_\mu}^2 \rangle < 1.2$ | 90% | [97] ^a |
| COHERENT + Dresden-II | w/o transition CR | $-7.1 < \langle r_{\nu_e}^2 \rangle < 5$ | 90% | This work ^c |
| | w transition CR | $-56 < \langle r_{\nu_e}^2 \rangle < 5$ | 90% | This work ^c |
| COHERENT + Dresden-II | w/o transition CR | $-5.9 < \langle r_{\nu_\mu}^2 \rangle < 4.3$ | 90% | This work ^c |
| | w transition CR | $-58.2 < \langle r_{\nu_\mu}^2 \rangle < 4.0$ | 90% | This work ^c |

^aCorrected by a factor of two due to a different convention, see ref. [21].

^bCorrected in ref. [93].

^cUsing the Fef quenching factor.

Table 7. Experimental limits for the neutrino charge radii.